

Excitation Functions of the Analyzing Power in $p\vec{p}$ Scattering from 0.45 to 2.5 GeV

M. Altmeier,¹ F. Bauer,² J. Bisplinghoff,¹ M. Busch,¹ K. Büber,² T. Colberg,² L. Demirörs,² O. Diehl,¹ H. P. Engelhardt,¹ P. D. Eversheim,¹ O. Felden,³ R. Gebel,³ M. Glende,¹ J. Greiff,² F. Hinterberger,¹ E. Jonas,² H. Krause,² T. Lindemann,² J. Lindlein,² R. Maier,³ R. Maschuw,¹ A. Meinerzhagen,¹ D. Prasuhn,³ H. Rohdjeß,¹ D. Rosendaal,¹ P. von Rossen,³ N. Schirm,² V. Schwarz,¹ W. Scobel,² H. J. Trelle,¹ E. Weise,¹ A. Wellinghausen,² and R. Ziegler¹

(EDDA Collaboration)

¹*Institut für Strahlen-und Kernphysik, Universität Bonn, D-53115 Bonn, Germany*

²*I. Institut für Experimentalphysik, Universität Hamburg, D-22761 Hamburg, Germany*

³*Institut für Kernphysik, Forschungszentrum Jülich, D-52425 Jülich, Germany*

(Received 14 April 2000)

Excitation functions $A_N(p_p, \Theta_{c.m.})$ of the analyzing power in $p\vec{p}$ elastic scattering have been measured with a polarized atomic hydrogen target for projectile momenta p_p between 1000 and 3300 MeV/ c . The experiment was performed for scattering angles $30^\circ \leq \Theta_{c.m.} \leq 90^\circ$ using the recirculating beam of the proton storage ring COSY during acceleration. The resulting excitation functions and angular distributions of high internal consistency have significant impact on the recent phase shift solution SAID SP99, in particular, on the spin triplet phase shifts between 1000 and 1800 MeV, and demonstrate the limited predictive power of single-energy phase shift solutions at these energies.

PACS numbers: 25.40.Cm, 13.75.Cs, 21.30.Fe, 24.70.+s

Proton-proton elastic scattering with projectile energies up to 800 MeV has been studied thoroughly in the past to an extent that there is now a comprehensive database [1] for the long and medium range parts of the nucleon-nucleon (NN) force. In particular, recent precision measurements at IUCF of rare spin observables for projectile energies $T_p \leq 450$ MeV [2–5] added valuable information. As a result the phase shift solutions (PSS) [1,6] show only little variation among each other in this energy regime [3,5,7].

Modern meson exchange potential models [8–11] provide adequate descriptions of the data up to the pion production thresholds. At higher energies probing smaller distances (<0.8 fm), however, genuinely new processes may occur involving the dynamics of the quark-gluon constituents. A related problem is the nature of the strong repulsive core of the NN interaction that prevents a close contact at low energies. Accordingly, proton-proton scattering at 0.45–2.5 GeV is ideally suited to sample the short range part of the NN interaction with spatial resolutions of about 0.15 fm and to study the role of the heavy meson exchange [12,13].

This was the main motivation to start the EDDA experiment. As a first result it provided [14] excitation functions $d\sigma/d\Omega(p_p, \Theta_{c.m.})$ of unpolarized pp scattering. Measurements were performed with an internal CH₂ fiber target in the recirculating COSY beam during acceleration from 450 MeV up to the flattop (2500 MeV). Addition of these internally consistent data to the SAID database [15] allowed one to extend the global PSS from 1.6 to 2.5 GeV [1]. Since then these experimental results as well as this solution SM97 have been frequently used, e.g., in [13,16]. It became apparent that further progress can only come from spin observables of NN scattering.

Recently analyzing powers have been measured at SATURNE [17,18] for pp scattering at about 30 discrete energies between 1795 and 2795 MeV and angles $\theta_{c.m.} \geq 60^\circ$. The results have been included for the PSS of the Saclay-Geneva group [19] and the new SAID [1] solution SP99. The difference of the global solution SP99 to the preceding one, SM97, is small in the energy regime of heavy meson exchange, because analyzing powers are still very scarce between 1000 and 1800 MeV projectile energy. To close this broad gap consistent data of high relative accuracy and sufficient overlap with the single energy data at lower [3–5] and higher [17,18] energies are needed. The technique applied previously by EDDA and, with a polarized beam, at KEK [20], is perfectly appropriate, provided protons of high and stable polarization are available. Here we report on our experiment using an internal, polarized atomic beam target and the EDDA detector modified to meet the increased demands for vertex reconstruction.

The EDDA detector shown in Fig. 1 in a schematic fashion consists of two cylindrical double layers covering 30° to 90° in $\Theta_{c.m.}$ for the elastic pp channel and about 82% of the full solid angle. The inner layers are composed of scintillating fibers (HELIX) of 2.5 mm diameter which are helically wound in opposing directions and connected to 16-channel multianode photomultipliers. The outer layers consist of 32 scintillator bars (B) which are mounted parallel to the beam axis. They are surrounded by scintillator semirings (R; FR). The scintillator cross sections were designed so that each particle traversing the outer layers produces a position dependent signal in two neighboring bars and rings. The resulting polar and azimuthal angular resolutions are about 1° and 1.9° FWHM. Combined with

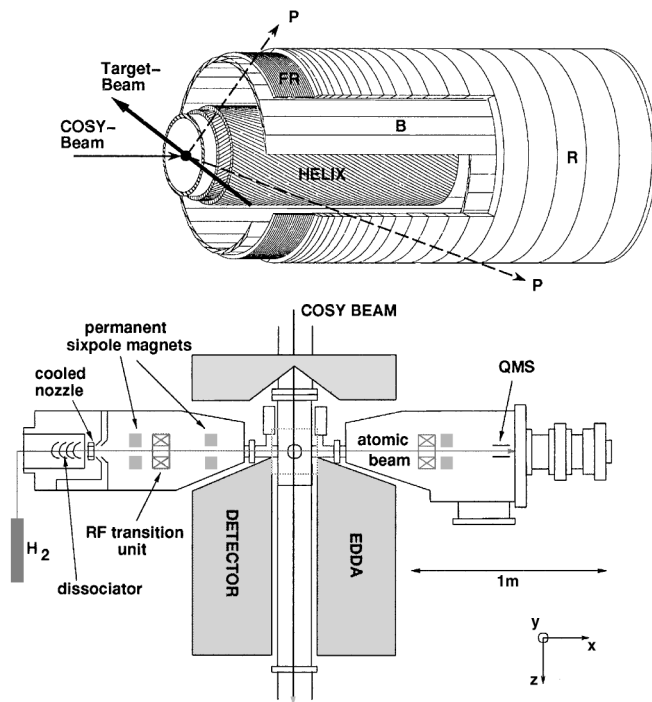


FIG. 1. Scheme of the EDDA detector (top) and its combination with the atomic beam target (bottom).

the spatial resolution of the HELIX fibers, this provides for vertex reconstruction with a resolution of better than 2 mm in the x , y , and z directions. Details are given in [21,22]. The beam parameters are continuously measured during the acceleration ramp. The beam momentum is derived from the rf of the cavity and the circumference of the closed orbit with an uncertainty of 0.25 to 2.0 MeV/ c for the lowest and the highest momentum, respectively. Beam position and width are deduced from the pp elastic scattering data. The horizontal and vertical beamwidths (FWHM) are about 3 and 5 mm, respectively.

The polarized target [23] is shown in Fig. 1, too. Hydrogen atoms with nuclear polarization are prepared in an atomic beam source with dissociator, cooled nozzle, permanent sixpole magnets and rf-transition units. The former removes one of the two electron spin states and the latter induces a transition to a depopulated hyperfine state. This preparation provides an atomic beam of ~ 12 mm width (FWHM) at the intersection with the COSY beam, a polarization of 85% in the center of the target beam, and an effective target thickness of 1.8×10^{11} atoms/cm². The magnetic holding field (B_x , $B_y \sim 10$ mT) across the fiducial vertex volume is corrected for ambient field components.

Measurements of the excitation functions $A_N(p_p, \Theta_{c.m.})$ were performed in cycles of about 13 s duration with data acquisition extending over the acceleration, the flattop at 3300 MeV/ c , and over the deceleration as well. With an average of 2.8×10^{10} protons in the ring, luminosities of about 8×10^{27} cm⁻² s⁻¹ were achieved and accumulated

to an integrated luminosity of $\sim 10^{34}$ cm⁻². The direction of the target polarization was changed cyclewise from $+x$ to $-x$, $+y$, and $-y$. The target was operating very stable and with constant polarization during each cycle as well as over run periods of up to two weeks. The two sets of runs with opposite polarizations, e.g., P_{+y} and P_{-y} , were combined to apply a correction for false asymmetries [24]. Indicating the number of events obtained simultaneously at the left [$N_L(\Theta)$] and the right side [$N_R(\Theta)$], we use $R = \sqrt{N_L N_{R+}}$ and $L = \sqrt{N_L N_{R-}}$ to calculate the left-right asymmetry $\epsilon_{LR} = (L - R)/(L + R)$ and then $A_N \cos\Phi = \epsilon_{LR}/P_y$ for the detector element in the azimuthal position Φ . The correction assumes the moduli of the polarizations $P_{\pm y}$ and the analyzing powers for the corresponding detector elements to be equal. Small deviations that may occur due to misalignments [$\delta A_N(\pm\Theta) \leq 0.04$] and improper spin flips ($\delta P_{\pm y} \leq 0.02$) influence ϵ_{LR} by at most 0.01% [20]. Similarly were the runs with $P_{\pm x}$ used to deduce A_N from the top-bottom asymmetries ϵ_{TB} .

The reduction of background takes advantage of the reconstructed vertex and the multiplicity patterns in both detector layers. Narrow cuts were applied to the hit patterns and to the vertex coordinate in the COSY beam (z) direction, a wider one in the xy plane around the beam profile (3σ limits) along an ellipse following the slow drift and shape variation of the COSY beam during acceleration. A fit of two proton trajectories to the hit pattern of an event under the constraint of elastic scattering kinematics is used to define a χ^2 criterion for a further event selection. The remaining background was estimated, guided by Monte Carlo simulations of elastic and inelastic pp interactions, to be mostly $\leq 2\%$ and only at highest energies and most backward angles up to 4.5%.

The absolute polarization values P_x and P_y are established in each running period with an integral normalization of the observed asymmetries $\epsilon(\Theta_{c.m.}) = P A_N(\Theta_{c.m.})$ for one momentum bin $\Delta p_p = 60$ MeV/ c around the energy $T_p = 730$ MeV ($p_p = 1380$ MeV/ c). The precise angular distribution $A_N(\Theta_{c.m.})$ from McNaughton *et al.* [25] is taken as a reference value.

The COSY beam changes its shape and position during acceleration and deceleration, though very reproducible in each cycle. Prior to merging all data in one final set it was necessary to perform consistency checks on subsets obtained under different conditions of polarization and acceleration cycles. Some of them are shown in Fig. 2; they demonstrate that the holding field is properly aligned to the detector coordinates (x, y), and that during acceleration and deceleration the same analyzing powers are obtained. This implies that vertex reconstruction and proper flip elimination of false asymmetries work well. Therefore all data were considered compatible and combined in one set. Altogether 3.1×10^7 elastic scattering events were collected.

Excitation functions $A_N(p_p, \Theta_{c.m.})$ with about 850 data points have been deduced from our experimental results by

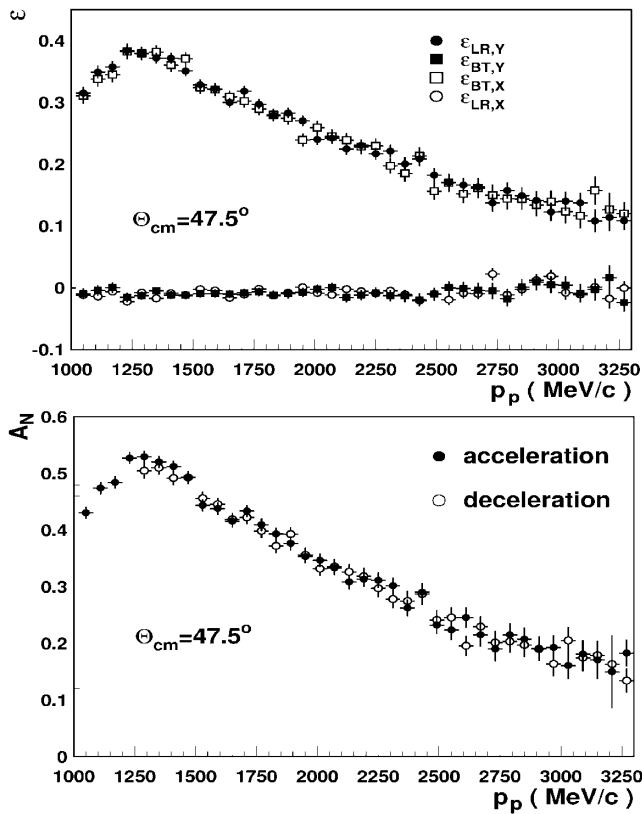


FIG. 2. Top: Asymmetries ϵ measured for a target polarization defined by a holding field in the y direction (solid symbols) or in the x direction (open symbols) during beam acceleration. Bottom: Analyzing powers A_N acquired during acceleration and deceleration, respectively. All data are for $\Delta\Theta_{c.m.} = \pm 5^\circ$ and $\Delta p_p = \pm 60$ MeV/c bins.

grouping them into $\Delta\Theta_{c.m.} = 4^\circ$ and $\Delta p_p = 30$ MeV/c wide bins. They are available upon request [26]. Here, five excitation functions are displayed in Fig. 3 using wider bins in $\Theta_{c.m.}$. For $\Theta_{c.m.} = 72.5^\circ \pm 0.5^\circ$ the discrete energy results from SATURNE [17,18] on the high as well as those from IUCF [4] on the low energy side are included to demonstrate the agreement with our data. Error estimates for A_N include contributions from the maximum deviations between data subsets ($\leq 2.1\%$), the polarization at the reference energy ($\leq 1.2\%$), and the impact of the background on the asymmetry (≤ 0.008). Errors due to the variation of the acting holding field with changes of the horizontal proton beam position during acceleration are negligible.

The comparison to the recent PSS SP99 [1] yields accordingly agreement in the general size and momentum dependence in the region of data overlap, but also systematic deviations in between, in particular, for momenta from 1800–2500 MeV/c; see Fig. 3. In this region A_N data are scarce in the present SAID database. For a first test of the impact the excitation functions A_N of this paper will eventually have on the scattering phases, we have added them to the present SAID database and searched for a global solution. It turns out that the χ^2 per data point

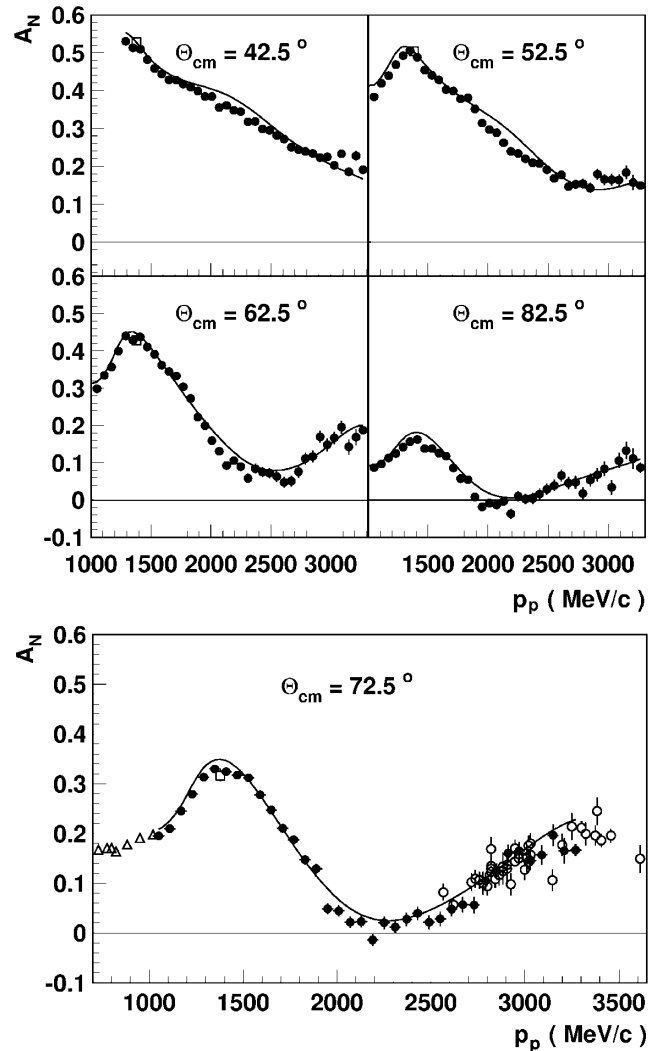


FIG. 3. Excitation functions $A_N(p_p, \Theta_{c.m.})$ for $\Delta p_p = 60$ MeV/c and $\Delta\Theta_{c.m.} = 5^\circ$ bins. Closed symbols, this experiment; open triangles (circles), data from [2–5] ([17,18]). The open squares indicate the normalization value for the effective target polarization at 1380 MeV/c [25]. The SAID solution SP99 is given as the solid line.

is not changed. At the same time the spin triplet phases, e.g., those of the 3F_2 partial wave shown in Fig. 4, experience significant changes. They are most prominent in the momentum range with the systematic deviations of our A_N data from solution SP99. This is due to the fact that the analyzing power times differential cross section is equal to the real part $\text{Re}(a^* \cdot e)$, where the invariant amplitudes a and e [27] include only triplet partial waves. The singlet partial waves in contrast have no preference for a particular spin orientation of a nucleon, because it is correlated to the opposite orientation of the second one to make a spin 0 state. This implies that the excitation functions for A_N are more sensitive to resonant excursions in triplet than to those in singlet partial waves [28]. However, the excitation functions measured here exhibit no evidence for energy-dependent structures, in agreement with the results

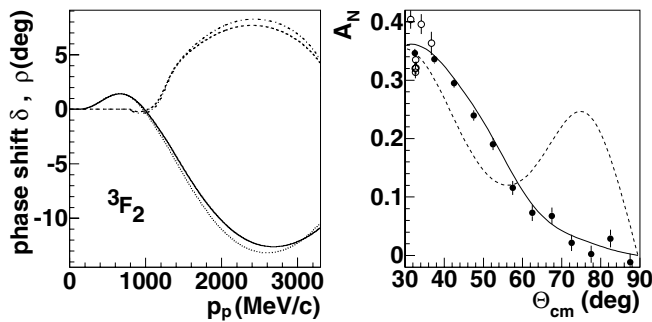


FIG. 4. Left: 3F_2 phase shifts. SAID solution SP99 is shown as the solid (real part) and the dashed (imaginary part) lines; the adjacent lines are obtained with our excitation functions A_N added to the database. Right: $A_N(\Theta_{c.m.})$ at $p_p = 2460$ MeV/c and the SES without (dashed line) and with (solid line) addition of the EDDA data (closed symbols) to the SAID database (open symbols).

of [29]. A more detailed discussion of sensitivities to and upper limits for such structures will be given in a forthcoming paper.

Starting from the global phase shift solution SP99, single-energy solutions (SES) can be searched for. Figure 4 shows the angular distribution $A_N(\Theta_{c.m.})$ around $p_p = 2460$ MeV/c in comparison to the SES prior to and after inclusion of our data. The two SES do not differ in χ^2 ; it is, however, obvious that the addition to before under-represented observables has a considerable impact on the SES and thus on *all* observables calculated with it.

In conclusion, we report on the first measurement of analyzing powers $A_N(p_p, \Theta_{c.m.})$ for $p\bar{p}$ scattering during acceleration in a recirculating synchrotron beam. The excitation functions agree with fixed energy data at 447 MeV and above 1795 MeV and close the broad gap in between with data of high precision and consistency. A first phase shift analysis including our data yields a global PSS for T_p up to 2.5 GeV showing distinct deviations from the current one, SP99, that occur mainly in the spin triplet phases. These deviations are even more pronounced in single-energy solutions and underline the limited predictive power of PSS as long as the database at these energies does not allow one to *unambiguously* determine the phase shift parameters [19,30]. Here, spin correlation parameters to be measured by the EDDA experiment next are needed.

The EDDA Collaboration gratefully acknowledges the great support received from the COSY accelerator group. Helpful discussions with and comments from R. A. Arndt,

E.L. Lomon, and R. Machleidt are very much appreciated. This work was supported by the BMBF, Contracts No. 06BN664I(6) and No. 06HH852, and by the Forschungszentrum Jülich, Contracts No. FFE 41126803 and No. 41126903.

-
- [1] R. A. Arndt *et al.*, Phys. Rev. C **56**, 3005 (1997), SAID solutions SM97 and SP99.
 - [2] W. Häberli *et al.*, Phys. Rev. C **55**, 597 (1997).
 - [3] F. Rathmann *et al.*, Phys. Rev. C **58**, 658 (1998).
 - [4] B. v. Przewoski *et al.*, Phys. Rev. C **58**, 1897 (1998).
 - [5] B. Lorentz *et al.*, Phys. Rev. C **61**, 054002 (2000).
 - [6] V. G. J. Stoks *et al.*, Phys. Rev. C **48**, 792 (1993).
 - [7] V. G. J. Stoks and J. J. de Swart, Phys. Rev. C **52**, 1698 (1995).
 - [8] V. G. J. Stoks *et al.*, Phys. Rev. C **49**, 2950 (1994).
 - [9] R. B. Wiringa *et al.*, Phys. Rev. C **51**, 38 (1995).
 - [10] R. Machleidt, K. Holinde, and Ch. Elster, Phys. Rep. **149**, 1 (1987).
 - [11] R. Machleidt, F. Sammarruca, and Y. Song, Phys. Rev. C **53**, R1483 (1996).
 - [12] R. Machleidt, Adv. Nucl. Phys. **19**, 189 (1989).
 - [13] R. Machleidt, *Progress Report of the Workshop on Intermediate Spin Physics, Jülich, 1998*, p. 169.
 - [14] D. Albers *et al.*, Phys. Rev. Lett. **78**, 1652 (1997).
 - [15] R. A. Arndt, I. I. Strakovsky, and R. L. Workman, Phys. Rev. C **50**, 2731 (1994).
 - [16] H. V. von Geramb *et al.*, Phys. Rev. C **58**, 1948 (1998).
 - [17] C. E. Allgower *et al.*, Phys. Rev. C **60**, 054001 (1999).
 - [18] C. E. Allgower *et al.*, Phys. Rev. C **60**, 054002 (1999).
 - [19] J. Bystricky, C. Lechanoine-LeLuc, and F. Lehar, Eur. Phys. J. C **4**, 607 (1998).
 - [20] Y. Kobayashi *et al.*, Nucl. Phys. **A569**, 791 (1994).
 - [21] J. Bisplinghoff *et al.*, Nucl. Instrum. Methods Phys. Res., Sect. A **329**, 151 (1993).
 - [22] M. Altmeier *et al.*, Nucl. Instrum. Methods Phys. Res., Sect. A **431**, 428 (1999).
 - [23] P. D. Eversheim *et al.*, Nucl. Phys. **A626**, 117c (1997).
 - [24] G. G. Ohlsen and P. W. Keaton, Nucl. Instrum. Methods **109**, 41 (1973).
 - [25] M. W. McNaughton *et al.*, Phys. Rev. C **41**, 2809 (1990).
 - [26] Access via <http://kaa.desy.de> and <http://www.iskp.uni-bonn.de/edda.html>.
 - [27] C. Lechanoine-Leluc and F. Lehar, Rev. Mod. Phys. **65**, 47 (1993).
 - [28] J. Lindlein, Ph.D. thesis, Universität Hamburg, 2000.
 - [29] R. Beurtey *et al.*, Phys. Lett. B **293**, 27 (1992).
 - [30] R. A. Arndt, I. I. Strakovsky, and R. L. Workman, nucl-th/0004039.